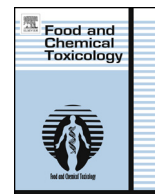




ELSEVIER

Contents lists available at ScienceDirect

Food and Chemical Toxicology

journal homepage: www.elsevier.com/locate/foodchemtox

In vitro-to-*in vivo* correlation of the skin penetration, liver clearance and hepatotoxicity of caffeine



M. Gajewska^{a,c,*}, A. Paini^a, J.V. Sala Benito^a, J. Burton^a, A. Worth^a, C. Urani^b, H. Briesen^d, K.-W. Schramm^{c,e}

^a Systems Toxicology Unit, EURL ECVAM, Institute for Health and Consumer Protection, European Commission, Joint Research Centre, Ispra, VA 21027, Italy

^b Department of Earth and Environmental Sciences, University of Milano Bicocca, Piazza della Scienza 1, Milano, Italy

^c Wissenschaftszentrum Weihenstephan für Ernährung, Landnutzung und Umwelt, Department für Biowissenschaften, TUM, Weihenstephaner Steig 23, Freising 85350, Germany

^d Wissenschaftszentrum Weihenstephan für Ernährung, Landnutzung und Umwelt, Lehrstuhl für Systemverfahrenstechnik, TUM, Weihenstephaner Steig 23, Freising 85350, Germany

^e Molecular EXposomics (MEX), Helmholtz Zentrum München – German Research Center for Environmental Health (GmbH), Ingolstädter Landstr.1, Neuherberg D-85764, Germany

ARTICLE INFO

Article history:

Received 4 August 2014

Accepted 14 October 2014

Available online 4 November 2014

Keywords:

Physiologically-Based Toxicokinetic (PBTK) modelling

Virtual cell-based assay

In vitro-to-*in vivo* correlation

Caffeine

ABSTRACT

This work illustrates the use of Physiologically-Based Toxicokinetic (PBTK) modelling for the healthy Caucasian population in *in vitro*-to-*in vivo* correlation of kinetic measures of caffeine skin penetration and liver clearance (based on literature experiments), as well as dose metrics of caffeine-induced measured HepaRG toxicity. We applied a simple correlation factor to quantify the *in vitro* and *in vivo* differences in the amount of caffeine permeated through the skin and concentration-time profiles of caffeine in the liver. We developed a multi-scale computational approach by linking the PBTK model with a Virtual Cell-Based Assay to relate an external oral and dermal dose with the measured *in vitro* HepaRG cell viability. The results revealed higher *in vivo* skin permeation profiles than those determined *in vitro* using identical exposure conditions. Liver clearance of caffeine derived from *in vitro* metabolism rates was found to be much slower than the optimised *in vivo* clearance with respect to caffeine plasma concentrations. Finally, HepaRG cell viability was shown to remain almost unchanged for external caffeine doses of 5–400 mg for both oral and dermal absorption routes. We modelled single exposure to caffeine only.

© 2014 The Authors. Published by Elsevier Ltd. This is an open access article under the CC BY-NC-SA license (<http://creativecommons.org/licenses/by-nc-sa/3.0/>).

List of symbols

$IVIV_{org}$ – *in vitro*- to- *in vivo* correlation factor for a given organ
 K_p – overall permeability coefficient for skin [cm/h]
 K_{pSC} – permeability coefficient in *stratum corneum* [cm/h]
 K_{pVE} – permeability coefficient in viable epidermis [cm/h]
 D_{SC} – diffusion coefficient in *stratum corneum* [cm²/h]
 D_{VE} – diffusion coefficient in viable epidermis [cm²/h]
 D_{HF} – diffusion coefficient in hair follicles [cm²/h]
 PC_{SC} – partition coefficient *stratum corneum*/vehicle
 PC_{VE} – partition coefficient *stratum corneum*/viable epidermis
 k_{form} – substance intake from formulation by *stratum corneum* [mL/h]
 MW – molecular weight [g/mol]

V_{max} – metabolic rate at maximum (saturating) substrate concentration [mg/h]
 K_m – substrate concentration at which the reaction rate is half of the maximal [mg/L]
 NEC – no-effect concentration [g/g_{cell}]
 kt – killing rates [1/h]
 cb – contaminant concentration inside cell [g/g_{cell}]
 fx – mass fraction of compartment x
 K_x – partition coefficient within cell
 n – number of moles
 r_{da} – uptake rate by a cell [L/m²/h]
 r_{ad} – elimination rate from a cell [L/m²/h]
 V – volume [L]
 W – wet weight [g]
 ρ – density [g/L]

* Corresponding author. Institute for Health and Consumer Protection, Systems Toxicology Unit, European Commission, Joint Research Centre, Via E. Fermi 2749, TP 126, Ispra I-21027, VA, Italy. Tel.: +39 0332 783955, fax: +39 0332 789963.

E-mail address: monika.gajewska84@wp.pl (M. Gajewska).

1. Introduction

Caffeine is found in varying quantities in the seeds, leaves, and fruits of some plants, especially coffee beans; therefore people are

mostly exposed to it via the diet on a daily basis. Not only is caffeine increasingly present in a number of food and beverages, it is also added to a growing number of cosmetics. It is used in many creams and lotions since it is believed to slow down the photoageing process of the skin and to absorb ultraviolet radiation, thereby preventing the development of tumours after skin exposure to sunlight. It is also used as an active compound in anti-cellulite products as it prevents excessive accumulation of fat in cells. As alkaloid, it has potent antioxidant properties. Caffeine increases the microcirculation of blood in the skin and also stimulates the growth of hair through inhibition of the 5- α -reductase activity (Herman and Herman, 2012).

Caffeine is rapidly absorbed from the gastrointestinal (GI) tract, and is almost completely metabolised in the liver, with 3% or less being excreted unchanged in urine. Its major metabolite, paraxanthine, which accounts for ca. 80% of caffeine bioconversion, is generated mostly by CYP1A2 activity. This enzyme is also responsible for the formation of other demethylated metabolites – theobromine (ca. 11%), theophylline (ca. 4%) and 1,3,7-trimethyluric acid (ca. 1%). These reactions, however, occur less efficiently, with the V_{\max}/K_m ratios 1–2 orders of magnitude lower than the case of paraxanthine. Different CYPs (2E1, 1A1) contribute to the liver bioconversion of caffeine (Carrier et al., 1988; Ginsberg et al., 2004; OECD SIDS, 2002; Regal et al., 2005). The metabolism, toxicokinetics of caffeine, and the use of this information in predictive modelling, have been described extensively in the literature (Csajka et al., 2005; Ginsberg et al., 2004; Lelo et al., 1986; Zandvliet et al., 2005).

There are many *in vitro* and several *in vivo* methods proposed in the literature for measuring absorption rate, percentage absorption and diffusion/permeation coefficients of caffeine through various skin sites and using vehicles such as water, ethanol, acetone, propylene glycol or mixtures of these solvents. Lehman et al. (2011) studied the difference between total absorption of caffeine through human skin *in vivo* and *in vitro* based on previously published data. They calculated the *in vitro/in vivo* (IVIV) ratio as the metrics for comparison. For harmonised data sets (in terms of the anatomical skin site, compound dose, vehicle composition and dose, length of exposure/wash time and the temperature) the average IVIV ratio was 0.96 (0.58–1.28). Chambin-Remoussenard et al. (1993) measured *in vivo* absorption of caffeine from two vehicles, an emulsion and an acetone solution, in 12 human volunteers. A surface recovery technique after a 6-h application of caffeine and a stripping method after a 30-min application were performed on the volar aspect of the forearm. The permeability coefficients with emulsion and acetone as solvents were $1.59 \cdot 10^{-04}$ and $9.53 \cdot 10^{-08}$ cm/h, respectively (ratio equals ca. 1700).

The internal concentrations of inhaled, dermally or orally absorbed substances are often predicted in animals and humans by means of Physiologically-Based Pharmacokinetic/Toxicokinetic (PBPK/PBTK) models. The use of PBTK models has increased significantly in the recent years, because of more accurate simulations of *in vivo* absorption, distribution, metabolism and excretion (ADME) processes in living organisms compared to classical kinetic models. The level of modelling complexity needed depends on the intended application and available biological information. The model predicts concentration-time profiles of a given compound at the organ level.

Cell-level toxicodynamics is described by the Virtual Cell-Based (VCB) assay; this model simulates processes in an *in vitro* system, especially the fate of a chemical within the well, taking into account partitioning with protein, lipids, and plastic binding (Zaldívar et al., 2010, 2011). The VCB consists also of a growth model with the cell growth phases (G1, S, G2, M phases). An additional feature takes into account the partitioning of compounds within the cell, and a toxicity model. The latter part of the model is based on two parameters: the no-effect concentration (NEC) and the killing rate (kt). The main simulated property is the intracellular concentration of a specific chemical within the cell and its corresponding effect

(cell viability). In order to link this effect with a specific external dose, it is necessary to join a PBTK model with the VCB composed of: the cell growth and division model, the cell partitioning model, the toxicity and effects models. Their integration, so called multi-scale modelling, allows *in vitro-to-in vivo* extrapolation (IVIVE) to be performed. The main objective of a multi-scale modelling is to study the methodology-based feasibility of overcoming the problems associated with the gaps between scales (i.e. cell and organ levels). This will allow to explore the continuum toxic effects and to establish an interface between different levels in terms of data and results transferability. The joint PBTK-VCB models describe the relationship between the tissue dose, early chemical–tissue interactions, and resulting toxic effect(s); they can be used to predict the toxicologically effective target organ dose. The HepaRG cell lines are a good candidate for these studies, since they are terminally differentiated hepatic cells derived from a human hepatic progenitor cell line that retain many characteristics of primary human hepatocytes, and thus the advantage of using these cells is that they are metabolically competent.

The goal of this study was to apply the caffeine PBTK model to: (i) correlate the *in vivo* and *in vitro* amounts of caffeine permeated through the skin, (ii) quantify the *in vivo* and *in vitro* differences in liver clearance and (iii) join the PBTK model with the VCB assay in order to associate external *in vivo* dose with *in vitro* HepaRG cell viability for oral and dermal absorption of caffeine. This work builds on and refines the PBTK model of caffeine used previously in oral-to-dermal extrapolation (Gajewska et al., 2014) to perform *in vitro-to-in vivo* correlation studies and present the concept of multi-scale modelling.

2. Materials and methods

In this work we used the available literature *in vivo* and *in vitro* caffeine experimental data to parameterise and validate the PBTK model and *in vitro* experimental results on HepaRG cell viability acquired at the Institute for Health and Consumer Protection, Joint Research Centre (JRC), Ispra, Italy, to calibrate the Virtual Cell-Based Assay model.

2.1. Experimental data used to calibrate and validate the PBTK model

2.1.1. Skin penetration

2.1.1.1.

In vivo. Table 1 shows *in vivo* literature studies of caffeine absorption as a percent of an absolute dose applied on the skin that were used to verify the *in vivo* simulations of the PBTK model (described below) in terms of its parameters such as caffeine intake from formulation (k_{form}) by *stratum corneum*, diffusion coefficients in *stratum corneum* (D_{sc}), viable epidermis (D_{ve}) and hair follicles (HF) (D_{HF}), partition coefficients between *stratum corneum*/vehicle (PC_{sc}), between *stratum corneum*/viable epidermis (PC_{ve}) and between hair follicles and vehicle (PC_{HF}).

In vivo plasma concentrations of caffeine following oral absorption were taken from: (i) Lelo et al. (1986) where a non-smoking male volunteer ingested only once 270 mg of caffeine in a gelatin capsule followed by 150 mL of water; (ii) Csajka et al. (2005) where caffeine was given orally in a gelatin capsule (200 mg of caffeine sulphate) to 16 subjects and in a commercial dietary supplement (a mixture containing 200 mg caffeine and 20 mg ephedrine alkaloids) to 8 subjects. For model validation, plasma concentrations from the oral study by Newton et al. (1981) were selected, in which a gelatin capsule containing 300 mg of caffeine was administered to one male subject. Plasma caffeine levels after dermal absorption were taken from Otberg et al. (2008). In this experiment caffeine in an ethanol/propylene glycol vehicle was administered to 6 male volunteers by applying the liquid onto a chest area of 25 cm² for 24 hours. In contrast to other dermal absorption studies, the additional impact of hair follicles in the overall absorption process was considered.

2.1.1.2.

In vitro. Table 2 provides some literature-derived *in vitro* results used to calibrate the PBTK model for simulating *in vitro* permeation profiles of caffeine. These studies were selected because all of them, in addition to absorption coefficients, report permeated amount of caffeine in time through the investigated type of human skin necessary for validation of the simulated *in vitro* permeation profile by the PBTK model. In the selected experiments, both full-thickness abdominal biopsies (Doucet et al., 1998) and excised human upper leg skin (Dias et al., 1999) were placed in Franz flow-through diffusion cells (1 cm²) to measure caffeine permeation into the receptor medium (continuously stirred). In the study of Wilkinson et al. (2006), breast

Table 1Literature data for *in vivo* caffeine permeation.

Reference	Dose/vehicle	Skin site/characteristic	% Of dose absorbed
Feldmann and Maibach (1970)	4 µg/cm ² over 13 cm ² in acetone	Forearm	47.56 (*)
Liu et al. (2011); Oberg et al. (2008)	Dose = 10 µg/cm ² Area = 25 cm ² in ethanol/propylene glycol	Chest	Open HF: 57.4 Closed HF: 36
Franz (1978)	4 µg/cm ² in 1:1 aq ethanol/acetone	Abdominal skin	22.1
Bronaugh and Franz (1986)	60 µg/cm ² in ethylene glycol gel; 0.5 µg/cm ² in petrolatum; 50 µg/cm ² in water gel	Abdominal skin	40.6 55.6 4
Lotte et al. (1993)	Area = 20–60 cm ² 1 Mmol/cm ² ¹⁴ C-labelled	Asian Black and Caucasian ethnic skin	1.06 1.01 and 0.96
Roskos et al. (1989)	21.7 g/L in aq. solution	Young (22–40 years) Old (>65 years)	48.2 25.2

* Based on urine recovery % dermal dose/% IV dose.

skin and abdominal skin (with dermis part removed) were mounted in PTFE Scott Dick flow through cells with exposed skin area of 0.64 cm² and continuously stirred receiver chamber.

2.1.2. Liver metabolism

Liver *in vitro* metabolism rates of caffeine taken from Ha et al. (1996) are shown in Table 3. They were measured in terms of recombinantly expressed enzymes V_{max}^{CYP} [pmol·h⁻¹·pmol CYP⁻¹]. A combination of human microsomal protein per gram liver (MPPGL) [mg_{protein}/g_{liver}] together with hepatic enzyme abundance (CYP_{content} [pmol CYP/mg_{protein}]) was used to scale data from recombinantly expressed enzyme systems (Barter et al., 2007). A correction for any difference in intrinsic enzyme activity from

that of the native enzyme in human liver would be additionally required once this information is available. V_{max} rates [mg/h/g_{liv}] provided in Table 3 were scaled according to:

$$V_{\max}^{\text{CYP}} \cdot \text{MW} \cdot 10^{-9} \cdot \text{CYP}_{\text{content}} \cdot \text{MPPGL}$$

Where:

$$\text{MPPGL} = 10^{(-0.3 \cdot \text{LogAge} + 2.04)}$$

where: Age = 21 (Lelo et al., 1986) giving MPPGL = 43.988.

(1)

Table 2Literature data for *in vitro* caffeine permeation (human skin).

Reference	Dose/vehicle	Human skin type	Diffusion coefficient (D [cm ² /h]); permeability coefficient (Kp [cm/h])	Partition coefficients	Max. abs. rate [µg/cm ² /h]	% Of dose absorbed
Wilkinson et al. (2006)	4 mg/mL in ethanol/water	Breast and abdominal skin from surgical waste full-thickness	–	–	1.75	17.3
Doucet et al. (1998)	260 mg/cm ² in O/W* and W/O/W* (ethylene oxide/propylene oxide + oil phase)	Abdominal biopsies	O/W:D _(SC+VE) = 3.85·10 ⁻⁶ W/O/W:D _(SC+VE) = 1.52·10 ⁻⁶	–	–	O/W: 3.21 W/O/W: 1.25
Dias et al. (1999)	25.82 mg/mL in water	Upper leg – isolated epidermis	K _{pVE} = 2.21·10 ⁻⁴ D _{SC} = 1.98·10 ⁻⁷	PC _{SC} = 1.79	–	–

* Emulsion formulas that differ in oil/water phases.

Table 3*In vitro* metabolism rates scaled per gram of liver.

Reference	Substance and dosing conditions	Investigated material	Scaled metabolism rates V _{max} [mg/h/g _{liver}] and Km [mg/L]
Ha et al. (1996)	Caffeine 0.05–2 mmol/L in sodium phosphate buffer pH = 7.4	Microsomal preparations from human β-lymphoblastoid cell lines Human cytochrome P-450 isoenzymes (CYPs) expressed in human B-lymphoblastoid cell lines: CYP1A1, 1A2, 2A6, 2B6, 2D6-Val, 2E1, 3A4; and microsomal epoxide hydroxylase (EH)	Caffeine to theobromine 1A1: V _{max} = 1.8·10 ⁻⁴ ; Km = 79.62 1A2: V _{max} = 0.001; Km = 31.07 2D6-Met: V _{max} = 0.023; Km = 3087.62 2E1: V _{max} = 1.7·10 ⁻⁴ ; Km = 279.63 Caffeine to theophylline 1A2: V _{max} = 4·10 ⁻⁴ ; Km = 48.55 2D6-Met: V _{max} = 0.052; Km = 2427.38 2E1: V _{max} = 1.2·10 ⁻⁴ ; Km = 163.12 Caffeine to paraxanthine 1A1: V _{max} = 6·10 ⁻⁴ ; Km = 114.57 1A2: V _{max} = 0.0103; Km = 36.90 2D6-Met: V _{max} = 0.046; Km = 2136.09 Caffeine to trimethyluric acid 1A1: V _{max} = 8·10 ⁻⁴ ; Km = 50.49 1A2: V _{max} = 7·10 ⁻⁴ ; Km = 52.43 2D6-Met: V _{max} = 0.017; Km = 1772.96 2E1: V _{max} = 0.001; Km = 201.96 3A4: V _{max} = 0.005; Km = 8932.74

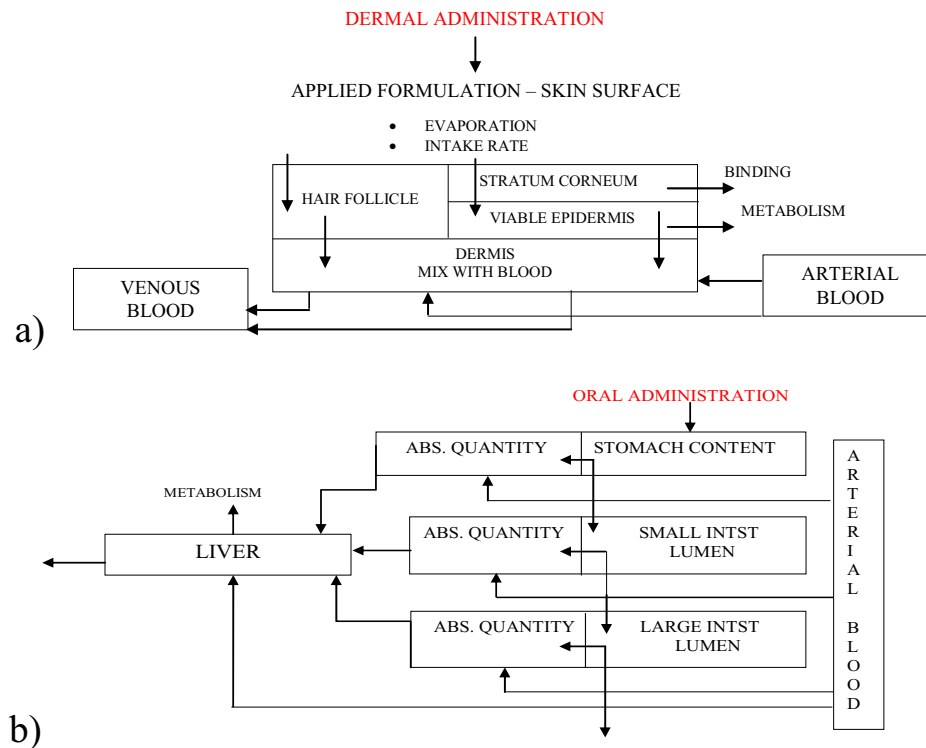


Fig. 1. *In vivo* skin (a) and GI tract (b) sub-compartments in PBTK model (Gajewska et al., 2014).

2.2. Experimental data used to calibrate the virtual cell-based assay

2.2.1. Chemical and cell line

Caffeine (58-08-2) was purchased from Fluka. Tetramethylrhodamine, ethyl ester (TMRE), Toto 3, and Hoechst 33342 were purchased from Invitrogen. Cryo preserved Human Cell Line HepaRG was obtained from INSERM's laboratory U522 and a cell culture bank had been established in house at the JRC (Mennecozi et al., 2011).

2.2.2. Viability in HepaRG assessed using Cellomics ArrayScan vTi

For the purpose of the current study, an in house experiment on HepaRG exposed to different concentrations of caffeine for 24 h was carried out to optimise the *in silico* VCB assay parameters: NEC and kt. The methodology was based on Mennecozi et al. (2011). Briefly, HepaRG cells were seeded at a density of 2.6×10^4 cells/cm² in a growth medium composed of Williams E medium supplemented with 10% Fetal Calf Serum (FCS), 100 units/mL penicillin, 100 µg/mL streptomycin, 5 µg/mL insulin, 2 mmol/L glutamine and 5×10^{-5} M hydrocortisone hemisuccinate. Further culturing was carried out for 2 more weeks with the same medium supplemented with 2% DMSO in 75 cm² culture flask. The medium was renewed every 2 to 3 days. After differentiation, HepaRG cells were detached by gentle trypsinisation, and then seeded at a density of $4-5 \times 10^4$ /well in 96 well microtiter plates (BD Biosciences) to allow the selection of hepatocyte-like populations. The cells were used for testing within one week after plate seeding. Caffeine was diluted in culture medium with 5% HyClone Fetalclone III serum. Eleven concentrations of caffeine, ranging from 0 mmol/L to 75 mmol/L, were tested, using 3 wells for each concentration (technical replicates). After 24 h of exposure, treated HepaRG cells were stained with TMRE, Toto 3, and Hoechst 33342 for 30 minutes. This assay was performed five times (biological replicates). Viability was assessed with a high-content analysis (HCA) approach using Cellomics ArrayScan vTi (Thermo Scientific, Pittsburgh, PA, USA). A 10x objective was used to collect 10 image fields per well for two fluorescence channels with the XF93 filter set. Cell count analysis was performed using the Target Activation Bioapplication v.4 from Cellomics Scan Software.

2.3. The PBTK model

The caffeine PBTK model for the healthy Caucasian population was previously described in Gajewska et al. (2014) and applied in simulating ADME profiles of caffeine after oral and dermal absorption. The model consists of gastrointestinal (GI tract) and skin sub-compartments (Fig. 1). In this work we used the dermal PBTK model for *in vitro*-to-*in vivo* correlation (IVIVC) of skin penetration and the oral PBTK model for IVIVC of liver clearance. Both models were used in predicting the liver cell (HepaRG) viability.

To better simulate the *in vitro* skin absorption the skin model was slightly modified and simplified to include two skin layers, *stratum corneum* and viable epidermis without hair follicles, and a receptor compartment instead of dermis (Fig. 2).

In modelling the following assumptions were additionally taken: (i) the absorption parameters including formulation uptake and diffusion coefficients were assumed constant in time; however diffusion and partition coefficients were different for *stratum corneum*, viable epidermis and hair follicles (if considered, *in vivo* case only); (ii) influence of different skin anatomical origin on permeation was neglected; (iii) inter-individual differences in skin permeation were neglected.

The parameters were optimised according to the Levenberg-Marquardt algorithm for nonlinear data fitting (Moré, 1978).

2.4. The virtual cell-based assay

As described in Zaldívar et al. (2010, 2011) the VCB assay integrates: (i) an *in vitro* fate and transport model that calculates the time-dependent chemical concentration in the medium as well as in the headspace; it takes into consideration a series of processes including evaporation, partitioning of chemicals from the dissolved phase to serum proteins and lipids, migration to the plastic, and also degradation and metabolism; (ii) a cell growth and division model that is based on a four stage-based approach (Gérard and Goldbeter, 2009), with each stage corresponding to one of the four cell cycle phases: G1, S, G2 and M (Zaldívar et al., 2010); (iii) the cell partitioning model that was built on the assumption that once the

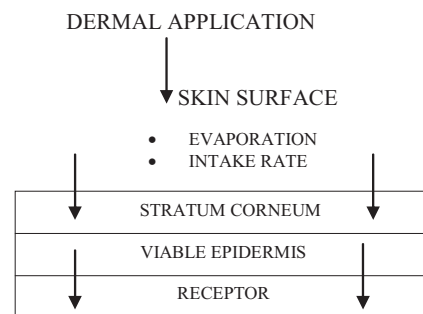


Fig. 2. Refined *in vitro* skin sub-compartments in the PBTK model.

Table 4
The parameters of VCB model.

Parameter type	Abbreviation used in the model	Value	Units	Ref.
Mass fraction of compartment f_x (aq-aqueous, l-lipids, p-proteins)	f_{aq}	0.72	% weight	Zaldívar et al. (2010, 2011)
	f_l	0.012		
	f_p	0.268		
Partition coefficient within a cell (l-lipids, p-proteins)	K_l	$1.63 \cdot 10^{-4}$	m^3/kg	
	K_p	1.36	m^3/mol	
Uptake rate	r_{da}	35.208	$L m^{-2} h^{-1}$	
Elimination rate	r_{ad}	35.208	$L m^{-2} h^{-1}$	
Wet weight	W	$1.79 \cdot 10^{-9}$	gr	
Volume of the cell	V	$1.67 \cdot 10^{-15}$	m^3	

chemical is taken up by the cell, a partitioning occurs between three compartments: one aqueous fraction and two non-aqueous fractions corresponding to structural components (proteins) and energy resources (lipids); and (iv) a toxicity and effects model which takes into account the direct effects of a chemical intracellular concentration, C_{cell} , on cell dynamics (survival/mortality) expressed by using the killing rate (k_t) and the no-effect concentration (NEC) (Billoir et al., 2007; Lopes et al., 2005). The mathematical equations of the Virtual Cell Based assay are reported in Zaldívar et al. (2010, 2011).

The PBTK and VCB models were joined via intracellular liver concentrations estimated by the PBTK model and then used to calculate the concentration inside the liver cells and their resulting viability. The detailed information about this joint model is provided in Appendix 1. The VCB model parameters together with their references are in presented in Table 4.

3. Results

3.1. In vitro-to-in vivo correlation of skin permeation

We carried out three calibration/modelling steps in determining IVIVC of skin penetration: (I) the *in vitro* skin model was optimised with respect to *in vitro* permeation results, (II) some of the *in vitro*-optimised parameters (namely diffusion coefficient in viable epidermis, partition coefficients in skin layers) were scaled up to *in vivo* values by the *in vivo* skin PBTK model based on caffeine plasma concentrations, (III) the $IVIV_{skin}$ ratio for skin penetration

was calculated (Equation 2) for the maximal permeated amount of caffeine estimated *in vitro* and *in vivo* using identical exposure scenarios for the *in vitro* and *in vivo* skin models.

$$IVIV_{skin} = \frac{A_{max, in vitro}}{A_{max, in vivo}} \quad (2)$$

The selected three literature *in vitro* studies were compared and absorption parameters were calibrated by the PBTK model fitting with respect to published permeated amounts of caffeine through the skin. The partition coefficient between *stratum corneum* and viable epidermis (PC_{VE}) was estimated by means of 10 literature Quantitative Structure–Property Relationships (QSPRs) (Gajewska et al., 2014) and the median value was chosen. Results are presented in Table 5. All the calibrated and estimated parameters (percentage of absorbed dose) by the model are in regular font, measured in bold, and QSPR-predicted are in italic.

Fig. 3 shows the simulated versus measured *in vitro* results for the literature experiments. In all the simulations we assumed 1 mL of applied solution on the skin surface and the same values of caffeine intake rate from a formulation (k_{form}) and viable epidermis parameters (D_{VE} , PC_{VE}) – the difference in using different vehicles was reflected only in modified *stratum corneum*/vehicle partition coefficients (PC_{SC}): 4 and 10 for water/oil/water (W/O/W) and oil/water (O/W) vehicles, 2.5 for ethanol/water and 1.79 for water.

In the second step of the correlation strategy, we used *in vivo* caffeine levels in plasma following skin absorption with open and closed hair follicles (Otberg et al., 2008) to optimise some of the parameters. Table 6 provides the final parameter values. D_{SC} , PC_{SC} and PC_{VE} (calculated by using QSPRs) were taken from *in vitro* studies of Wilkinson et al. (2006) because the vehicle was similar (ethanol/water vs. ethanol/propylene glycol). The remaining parameters: D_{HF} , D_{VE} , k_{HF} and k_{form} were optimised because of obviously different permeation properties of viable epidermis *in vivo* (when linked to dermis and blood flow) and enhanced action of follicles not considered in the *in vitro* experiment. We assumed partition coefficient between hair follicles and solvent to be equal to 1 because of lack of information about it. Simulated versus experimental concentration-time points are shown in Fig. 4 for a male

Table 5
PBTK model optimisation of *in vitro* parameters (measured in bold, QSPR-predicted in italic, optimised/simulated in regular font).

Reference	Dose	% Of dose abs.	D_{SC} , D_{VE} [cm^2/h]	PC_{SC} , PC_{VE}	k_{form} [mL/h]
Doucet et al. (1998)	260 mg/cm ² 1% sol. Area = 1 cm ²	0.09 (W/O/W)* 0.216 (O/W)*	$D_{(SC+VE)} = 1.52 \cdot 10^{-6}$ (WOW) $D_{(SC+VE)} = 3.85 \cdot 10^{-6}$ (OW)	$PC_{SC} = 4$ (W/O/W) $PC_{SC} = 10$ (O/W) $PC_{VE} = 0.6$	0.06
Wilkinson et al. (2006)	4 mg/mL Area = 1.5 cm ² in ethanol/water	173 (opt.16.211)	$D_{SC} = 1.40 \cdot 10^{-7}$ $D_{VE} = 1.10 \cdot 10^{-6}$	$PC_{SC} = 2.5$ $PC_{VE} = 0.6$	0.06
Dias et al. (1999)	25.82 mg/mL water Area = 1 cm ²	0.455	$D_{SC} = 1.98 \cdot 10^{-7}$ $D_{VE} = 1.1 \cdot 10^{-6}$	$PC_{SC} = 1.79$ $PC_{VE} = 0.25$	0.06

* Emulsion formulas that differ in oil/water phases.

Table 6
PBTK model optimisation of *in vivo* parameters (taken from *in vitro* studies in bold).

Reference	Dose	% Of dose abs.	Diffusion coefficients [cm^2/h]	Partition coefficients	k_{form} [mL/h]
Otberg et al. (2008)	0.250 mg in 0.06 mL Ethanol/propylene glycol	Open HF = 87.11 Closed HF = 75.153	$D_{SC} = 1.40 \cdot 10^{-7}$ $D_{VE} = 1.50 \cdot 10^{-5}$ $D_{HF} = 1.24 \cdot 10^{-5}$	$PC_{SC} = 2.5$ $PC_{VE} = 0.6$ $PC_{HF} = 1$	$k_{form} = 0.2$ $k_{HF} = 0.153$

HF = hair follicles.

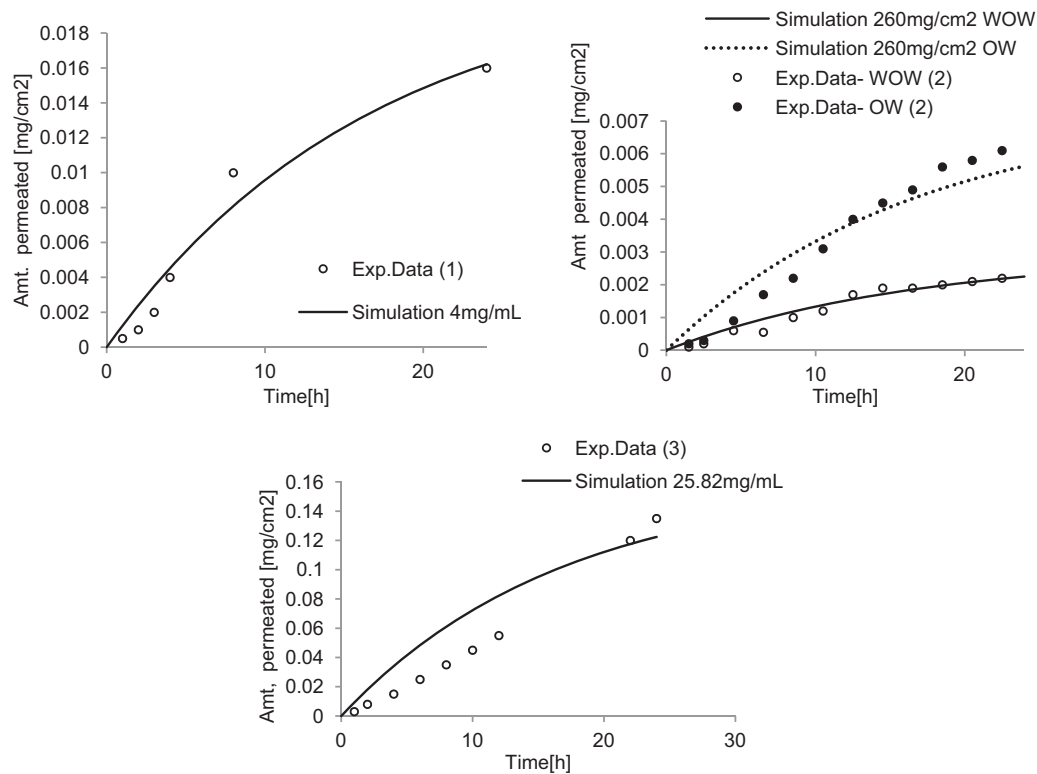


Fig. 3. Simulated (*in vitro*) amount of caffeine permeated through the skin over 24 h: (1) Wilkinson et al. (2006), (2) Doucet et al. (1998), (3) Dias et al. (1999).

subject (body weight = 75 kg). The *in vivo* PBTK model uses different percentage of skin available for permeation from 100% with open hair follicles to 80% with closed hair follicles according to optimisation results best fitting the experimental values.

In the third and final step, *in vitro*-to-*in vivo* correlation of permeated amount of caffeine in time was performed for the experimental design of Otberg et al. (2008) with 4 h of exposure to caffeine (*in vitro* parameters of Wilkinson et al. were used). Fig. 5 shows the permeation differences in *in vitro* and *in vivo* model simulations. *In vivo* results are ca. 6–9 times higher than *in vitro* estimates. The $IVIV_{\text{skin}}$ ratio based on the maximal permeated amount to receptor was equal to 0.133 for absorption with open follicles and 0.177 for absorption with closed follicles.

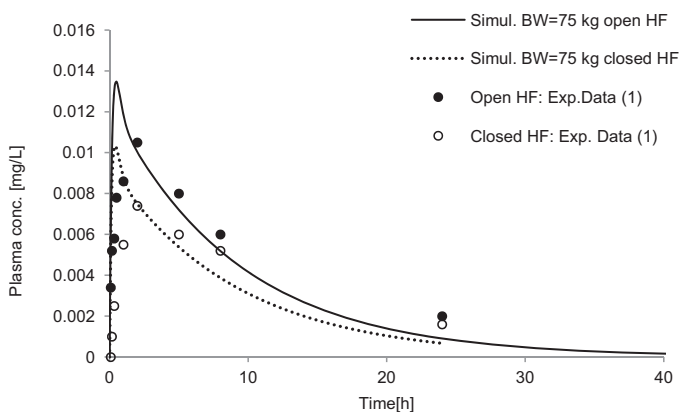


Fig. 4. Plasma concentrations of caffeine after *in vivo* dermal absorption: experimental data from (1) (Otberg et al. 2008) (HF = hair follicles).

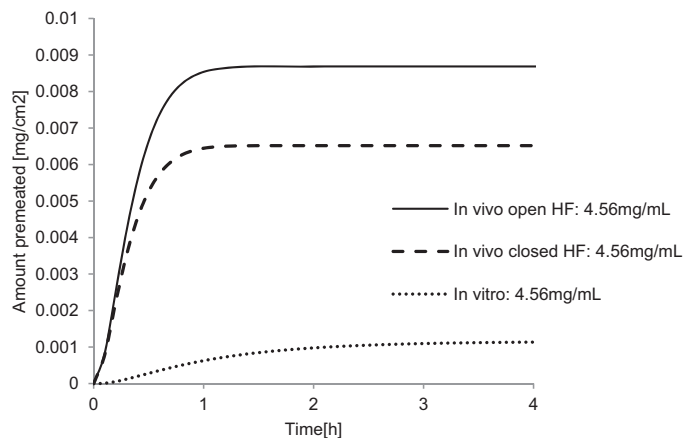


Fig. 5. *In vitro*-to-*in vivo* correlation of caffeine permeation (HF = hair follicles).

3.1.1. Skin metabolites

In principle, metabolism can also occur in skin but since no experimental sources were found, we used the OECD QSAR toolbox¹ (v3.1) to generate potential skin metabolites of caffeine. Skin metabolism simulator mimics the metabolism of chemicals in the skin compartment and contains a list of hierarchically ordered principal transformations, which can be divided into two main types – rate-determining and non-rate-determining. The rate-determining transformations are Phase I and Phase II, such as C-hydroxylation, ester hydrolysis, oxidation, glutathione conjugation, glucuronidation,

¹ <http://www.qsartoolbox.org/> (last accessed: 07.10.2014).

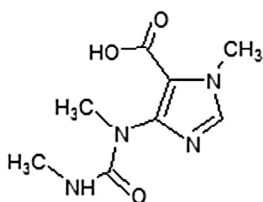


Fig. 6. QSAR toolbox predicted skin metabolite (caffeidine acid) of caffeine (not considered in the PBTK and VCB model simulations).

sulphonation. The non-rate-determining transformations include molecular transformations of highly reactive intermediates. The simulator starts by matching the parent molecule with the reaction fragments associated with the transformation having the highest probability of occurrence. This produces a set of first level metabolites. Each of these derived metabolites is then submitted to the same list of hierarchically ordered transformations to produce a second level of metabolites. The procedure is repeated until a constraint for metabolism propagation is satisfied (e.g. low probability of obtaining a metabolite or application of Phase II reaction (Dimitrov et al., 2005)). The only resulting structure of potential caffeine metabolite was caffeidine acid (CAS# 54536-15-1); see Fig. 6. The 6-membered ring opening is achieved through the hydrolysis of the amide in alkaline environment. However, no experimental studies yet exist to confirm that this chemical species is indeed generated in human skin. Moreover, caffeidine acid could not be found in liver metabolism experiments or generated through liver metabolism simulators. It was only found in microbial simulators and dedicated chemical reactivity simulations (basic hydrolysis). With no proof of the formation of the metabolite in humans, we did not consider it in the PBTK model simulations.

According to the authors of the model, very few experimental data were available for skin metabolism. Therefore, expert judgement was asked to confirm the probabilities of the metabolic reactions to occur. While the predicted reaction for caffeidine acid is a simple hydrolysis of an amide that may have been introduced in the model, it is not likely to occur since it requires a basic pH whereas the skin pH is slightly acidic.

3.2. In vitro-to-in vivo correlation of liver clearance

In this section we correlated the resulting *in vitro* and *in vivo* differences in liver clearance of caffeine by means of a novel $IVIV_{liver}$ factor based on the ratio between liver Area under Curve (AUC) *in vitro*-to-*in vivo* (Equation 3).

$$IVIV_{liver} = \frac{AUC_{liv, in vitro}}{AUC_{liv, in vivo}} \quad (3)$$

Liver metabolism rates (Michaelis–Menten parameters: V_{max} , K_m) for caffeine determined in *in vitro* experiments were scaled to the liver level and overall liver clearance rate in terms of V_{max}/K_m was calculated as the sum of all enzyme contributions. This sum was equal to 0.912 L/h. Independently, the *in vivo* liver clearance was calibrated by fitting the PBTK model to available *in vivo* plasma concentrations, which resulted in 10 L/h. The latter value represents average fitting results with respect to 1–16 subjects receiving a single oral dose of caffeine (Csajka et al., 2005; Lelo et al., 1986) and validated for a similar oral absorption study (Newton et al., 1981) and dermal absorption experiment performed on 6 subjects with mean results published (Otberg et al., 2008).

Fig. 7 shows liver concentrations of caffeine with *in vitro*-derived and *in vivo*-fitted caffeine clearance rates. In this case, oral

dosing conditions of 270 mg of caffeine in a gelatin capsule (Lelo et al., 1986) was used for an average body weight of 83 kg. Independently, both *in vitro* and *in vivo* parameters were used in the oral PBTK model to simulate concentration-time profiles of caffeine in the liver. The $IVIV_{liver}$ value was estimated to be ca. 2.3.

3.3. HepaRG cell viability

Finally, the PBTK model-estimated concentrations in the liver following oral and dermal single exposure conditions (doses: 5–400 mg, concentration: 4.25 mg/mL, skin area: 25–2400 cm²) were used as input parameters to the VCB model that estimated concentration inside cells and HepaRG cell viability. We chose the upper dosing range to be ca. 2 times higher than the No-Observed Adverse Effect Level (NOAEL) extrapolated for humans from experimental rat studies (Gajewska et al., 2014). The cell viability measured *in vitro* was assumed to be identical to the *in vivo* situation. Experimental *in vitro* viability data showed that caffeine exposure to HepaRG for 24 h produced a statistically significant reduction of cell viability at caffeine concentrations higher than 3 mM. This concentration–response curve (Fig. 8) was used to optimise the VCB assay parameters, the no-effect concentration and killing rate, to minimise the error in model prediction, in a single exposure mode for the HepaRG cell line. This resulted in the following optimised values of NEC and k_t : NEC = 0 g/g_{cell}, k_t = 0.222 1/h.

The human PBTK models for dermal and oral absorption of caffeine were modified for new dosing conditions but maintaining a constant dermal concentration of 4.56 mg/mL in ethanol/propylene glycol vehicle (Otberg et al., 2008) and with caffeine release from a gelatin matrix in the GI tract (Lelo et al., 1986). The dermal simulation was based on the open hair follicles case, with the solution being administered to the skin for 4 h.

Concentration inside the cells is quantified as milligram per gram (mg/g_{cell}) of HepaRG cells. Furthermore, the number of cells in the *in vitro* system was scaled up to total liver by using a factor of 23·10⁶ cells/g liver, and assuming a 1.5 kg liver, what resulted in 34,500·10⁶ cells. The latter value was used for simulation of the cell viability whose results are listed as percentage in Table 7. This table contains also the peak concentrations (C_{max}) in the liver and inside cells calculated by the PBTK and VCB models respectively.

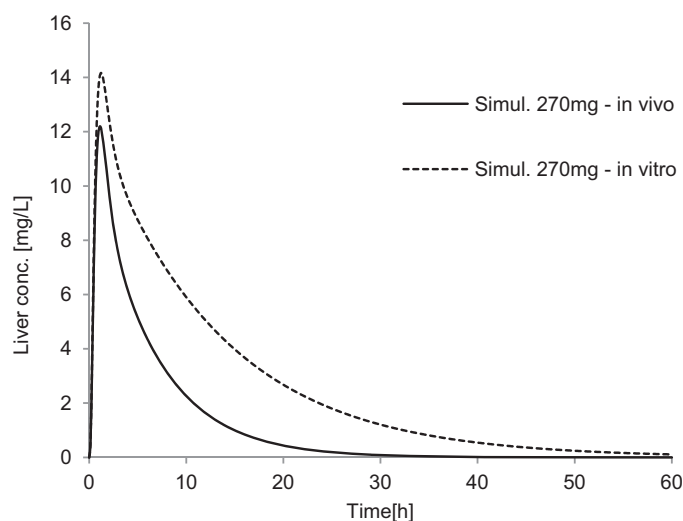


Fig. 7. Caffeine concentrations in liver using *in vitro* and *in vivo* optimised parameters. Oral dosing conditions according to Lelo et al. (1986).

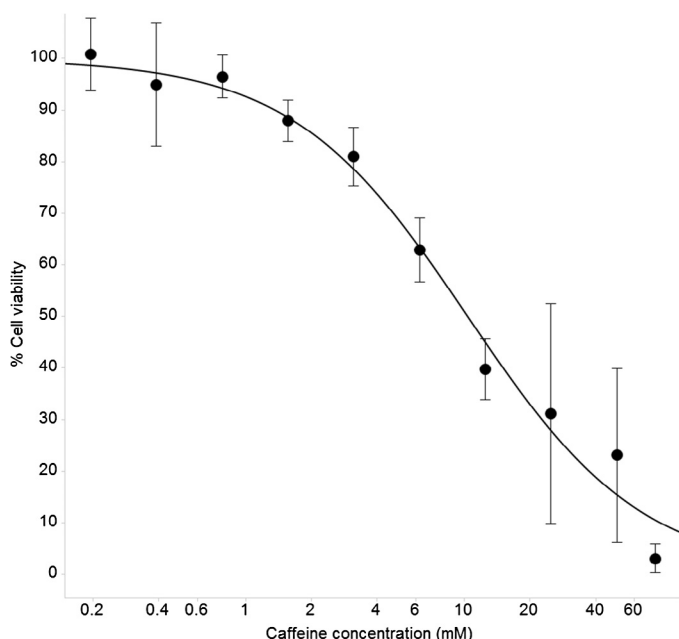


Fig. 8. Caffeine effect on cell viability of HepaRG cell line (using 5 biological replicates). The plot (x scale in log units) and curve fitting (logistic regression) was performed with TIBCO Spotfire 6.0.1.

Fig. 9 presents the relationship between the HepaRG cell viability and the external doses. Even for the two highest analysed external doses of 300 and 400 mg (4.00 and 5.33 mg/kg BW for a 75-kg man) the simulated decrease in cell viability is insignificant.

4. Discussion

In this work three different approaches have been illustrated for *in vitro*-to-*in vivo* correlation studies. For skin permeation we calibrated independently *in vivo* and *in vitro* skin models with respect to selected experimental data from the literature. In particular, *in vitro* data from Wilkinson et al. (2006) for caffeine in an ethanol/water vehicle and Doucet et al. (1998) with specially prepared W/O/W and O/W vehicles were very well estimated by the PBTK model. The experimental results from Dias et al. (1999) were slightly

Table 7
Link of PBTK dermal model to the VCB-estimated cell viability.

Dermal external dose [mg]	C_{\max} liver [mg/L]	C_{\max} in liver cells [mg/g _{cell}]	Simulated cell viability [%]
0	Oral: 0 Dermal: 0	Oral: 0 Dermal: 0	Oral > 99.99 Dermal > 99.99
5	Oral: 0.187 Dermal: 0.050	Oral: $1.18 \cdot 10^{-10}$ Dermal: $1.46 \cdot 10^{-7}$	
10	Oral: 0.380 Dermal: 0.179	Oral: $2.36 \cdot 10^{-10}$ Dermal: $4.41 \cdot 10^{-7}$	
25	Oral: 0.984 Dermal: 0.389	Oral: $5.92 \cdot 10^{-10}$ Dermal: $1.02 \cdot 10^{-6}$	
50	Oral: 2.074 Dermal: 0.753	Oral: $1.19 \cdot 10^{-9}$ Dermal: $2.72 \cdot 10^{-6}$	
100	Oral: 4.464 Dermal: 1.402	Oral: $2.44 \cdot 10^{-9}$ Dermal: $9.73 \cdot 10^{-6}$	
200	Oral: 9.705 Dermal: 2.215	Oral: $5.15 \cdot 10^{-9}$ Dermal: $3.72 \cdot 10^{-5}$	
300	Oral: 15.175 Dermal: 3.929	Oral: $8.34 \cdot 10^{-9}$ Dermal: 0.0004	
400	Oral: 20.760 Dermal: 5.700	Oral: $1.23 \cdot 10^{-8}$ Dermal: 0.0016	

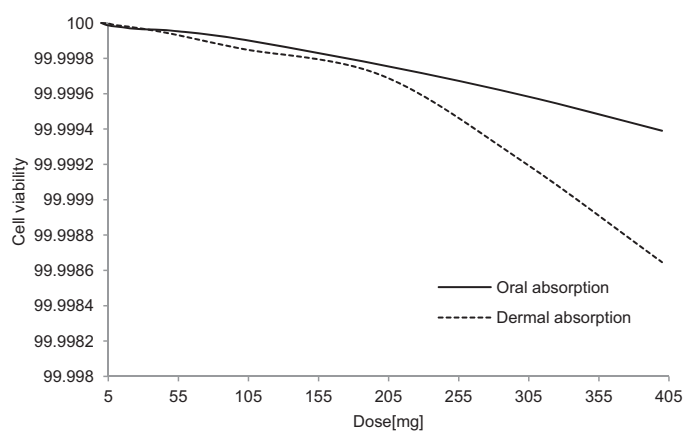


Fig. 9. PBTK/VCB simulations of cell viability as a function of external dose of caffeine applied dermally and orally for a male subject (BW = 75 kg).

less well simulated, probably due to the fact that measured permeation was through a layer of extracted viable epidermis, whereas the *in vitro* PBTK model took into account two skin layers. *In vivo* permeation (Otberg et al., 2008) was already concluded in the literature to be higher than the *in vitro* one following the same exposure settings such as concentration of caffeine, skin area, and exposure time (Liu et al., 2011). This is probably because the *in vitro* skin model under-predicts the amount absorbed due to experimental factors such as the permeability of the extracted part of the skin, the experimental temperature and the relatively semi-static conditions (periodical renewal of the acceptor medium) when compared to the *in vivo* situation, in which the systemic circulation provides a continuous perfusion of the skin compartment. We further applied the PBTK model to various experimental literature data (see Tables 1 and 2) to confirm this observation and to calculate a correlation factor ($IVIV_{\text{skin}}$). This is important when *in vitro* experimental results are to be used to establish safe external exposure levels and margins of safety for a given substance.

In comparison to skin permeation, $IVIV$ of liver metabolism is more complex. We used plasma concentrations as a surrogate for missing *in vivo* liver concentrations to calibrate *in vivo* liver clearance and then we analysed the *in vitro*-*in vivo* difference in liver concentration-time profiles to perform the correlation. We believe that using AUC in this case is more appropriate than using C_{\max} as it better reflects kinetic differences in the elimination phase – for lower metabolic clearance rates, the half-life is higher and the compound stays longer in the body, which may result in different toxicological responses and bioaccumulation. We limited our studies to oral absorption because, in general, it gives higher internal concentrations of absorbed chemicals when compared to dermal intake, and thus shows clearer differences in liver clearance. Calibration resulted in the *in vivo* clearance being ca. 10 times faster when compared to the *in vitro*-derived one based on CYP1A2, CYP1A1, CYP2D6-Met and CYP2E1 metabolism rates (Ha et al., 1996). We did not consider inter-individual differences in enzyme activities which would result in different clearance rates and consequently different $IVIV_{\text{liver}}$ ratios. There are many factors that contribute to inter-individual differences in total activity of specific enzymes and drug metabolism rates that are dependent on this. The maximum total activity of biotransformation enzymes is dependent on many factors such as genetic polymorphisms, prior (enzyme induction) or concomitant (enzyme stabilisation and reversible or irreversible inhibition) exposure to drugs and environmental chemicals, presence or depletion of cofactors, dietary factors, diseased states, epigenetic factors and endogenous hormonal factors, which

change with age and differ between male and female subjects (Venkatakrishnan et al., 2000).

Finally a dose–response curve was generated by linking the PBTK model output (liver C_{max}) with the VCB model. This allows the application of both forward and reverse dosimetry. The forward approach means that when exposed to a given external dose, the joint model predicts the corresponding effect on liver cell viability. The backward approach can be used to estimate from a given cell viability the corresponding external dose. Concentrating on the forward dosimetry approach, we found almost no effect of caffeine on HepaRG cell viability (reduction of cell viability by much less than 1%) for doses up to 400 mg. Caffeine is known to be extensively metabolised in the liver *in vivo* but the main organs affected are the brain and heart. Simulated dose–response profiles following dermal and oral caffeine absorption were similar, even though maximal liver concentrations determined by the PBTK model after oral exposure were higher (see Table 7, second column). We used only single doses of up to 5.33 mg/kg BW which was more than ca. 2 times the extrapolated oral NOAEL from rat studies – 2.1 mg/kg BW (for a body weight of 75 kg). Compared to our simulations, experimental *in vitro* results showed a significant decrease in HepaRG cell viability at much higher doses. Fig. 8 shows that a caffeine concentration of ca. 2 mmol/L (=388.4 mg/L) produces 20% of viability loss. The maximal liver concentration that was applied as an input to VCB model was 20.76 mg/L following oral absorption of 400 mg. In addition, we used the PBTK dermal model with enhanced penetration via hair follicles regardless of the fact that while increasing the external absolute dose, we also increased proportionately the skin area. In this way, we showed that an extreme case of caffeine skin absorption still produced lower liver C_{max} values when compared to the oral case. However, interestingly, the concentration inside the cells and their viability calculated by the VCB model revealed that dermal exposure led to a slightly faster decline in cell viability (regeneration of liver cells was not simulated). This may be due to the prolonged exposure of liver to caffeine after skin absorption as the compound enters the circulation gradually and therefore stays in the body for a longer time.

In conclusion, model-based correlation studies of single dose exposures to caffeine indicated that *in vitro* skin permeation of caffeine is ca. 6–9 times lower than *in vivo* simulated values and, in a similar manner, *in vitro*-derived liver clearance is ca. 10 times slower than fitted *in vivo* clearance. Finally, the multi-scale modelling approach (PBTK + VCB models) revealed almost no effect of caffeine after oral and dermal absorption (up to 5.33 mg/kg BW) on the viability of liver (HepaRG) cells regardless of the absorption route. Dermal absorption produced, however, a slightly higher observable effect than the corresponding oral absorption of the same single doses in the investigated range. The approaches described in the present paper provide a promising means of performing *in vitro*-to-*in vivo* correlations that may contribute to the chemical risk assessment process.

Conflict of interest

The authors declare that there are no conflicts of interest.

Transparency document

The Transparency document associated with this article can be found in the online version.

Acknowledgements

This research was partially funded by the Seventh Framework Programme (FP7/2007–2013) COSMOS (Integrated In Silico Models for the Prediction of Human Repeated Dose Toxicity of Cosmetics to Optimise Safety) Project and by Cosmetics Europe.

Appendix 1

Joint modelling approach: PBTK and VCB

The PBTK model calculates the internal concentration of caffeine on organ level in the human body following a specified exposure scenario. The simulated liver concentrations of caffeine in time are assumed to be a concentration outside the hepatic cells (HepaRG). Using mass balance equations, the concentration of the chemical inside the cells is calculated by the VCB model (Zaldivar et al. (2010, 2011)). The cell model consists of 3 compartments (lipid, protein and aqueous). The interchange of the chemical through the cell membrane occurs via diffusion and then the chemical is distributed into the 3 compartments of the cell by its partitioning. In the present work the chemical was uptaken by passive diffusion; however, it is important to highlight that the cell membrane, which is an important compartment hosting relevant receptors, was not exploited in its full potential but it will be addressed in future work. When the chemical enters into the cell, a toxicokinetic process occurs which is governed by two parameters: No-effect Concentration (NEC) and killing rate (kt) (Fig. A1.1). These parameters are calculated and optimised to predicted cell viability via the VCB model using the *in vitro* experimental results.

The total number of moles of a compound in the cell is their sum in the different compartments:

$$n_{tot} = n_{aq} + n_p + n_L = (V_{aq} \cdot C_{aq} + V_p \cdot C_p + V_L \cdot C_L) \quad (A1.1)$$

where: the V_{i_s} refer to the compartment volumes and the C_{i_s} refer to the compartment's concentration [$\text{mol} \cdot \text{L}^{-1}$]. Also the total number of moles of a chemical can be expressed as:

$$n_{tot} = W \cdot C_b / MW \quad (A1.2)$$

where W is the cell weight [g], MW is the molecular weight of the chemical [$\text{g} \cdot \text{mol}^{-1}$] and C_b is the chemical concentration in the cell [$\text{g} / \text{g}_{cell}$]. The chemical is assumed to be in equilibrium between the different compartments with fixed values partition coefficients: $K_p = C_p / C_{aq}$ and $K_L = C_L / C_{aq}$.

The time evolution of this substance in the cell can be calculated by a simple mass balance, assuming that the uptake and elimination rates r_{ad} and r_{da} [$\text{L} \cdot \text{m}^{-2} / \text{h}^{-1}$] are proportional to the surface area of the cell (passive diffusion) and the transfer occurs through the aqueous compartment only as:

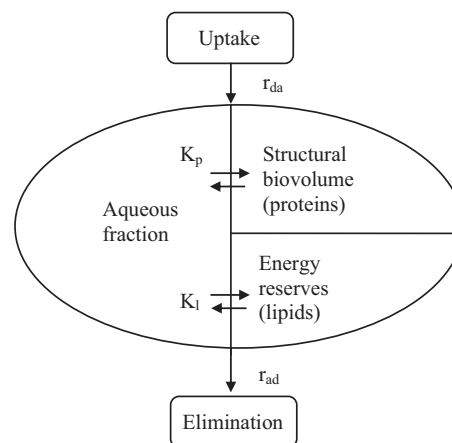


Fig. A1.1. Representation of the cell partitioning model. Once a chemical is uptaken in the cell it partitions between 3 compartments and is then eliminated (by excretion from the cell).

$$\frac{dn_{tot}}{dt} = V^{2/3} \cdot k' \cdot (r_{da} \cdot C_{diss} - r_{ad} \cdot C_{aq}) \quad (A1.3)$$

where C_{diss} and C_{aq} refer to the chemical concentration [$\text{mol}\cdot\text{L}^{-1}$] ($C_{diss} = C_{iv}/MW/1000$) outside of the cell (given by PBKT model) and in the aqueous compartment of the cell [$\text{mol}\cdot\text{L}^{-1}$], respectively; k' and V are constant and the volume of the cell as defined in Zaldívar et al. (2010, 2011). Applying the product rule of derivation to Equation A1.2 we get:

$$\frac{dn_{tot}}{dt} = \frac{1}{MW} \left(W \frac{dC_b}{dt} + C_b \frac{dW}{dt} \right) \quad (A1.4)$$

By rearranging the terms we obtain:

$$\frac{dC_b}{dt} = \frac{MW \cdot V^{2/3}}{W} (r_{da} \cdot C_{diss} - r_{ad} \cdot C_{aq}) - \frac{C_b}{W} \frac{dW}{dt} \quad (A1.5)$$

The latest term represents the dilution due to growth of the cell that in the case of HepaRG can be neglected.

Since the concentration in the aqueous fraction C_{aq} is not a value that is measured, then we have to convert in terms of C_b using the partitioning approach. The cell wet weight, W , can also be expressed as a function of the volumes of the different compartments:

$$W = \rho \cdot V = \rho(V_{aq} + V_p + V_L) \quad (A1.6)$$

On the other hand:

$$V_p = W_p / \rho_p; V_L = W_L / \rho_L; V_{aq} = W_{aq} / \rho_{aq} \quad (A1.7)$$

where W_p , W_L and W_{aq} are the masses of proteins, lipids and aqueous compartments in the cells and ρ_p , ρ_L and ρ_{aq} are their densities.

To find the correlation between C_{aq} and C_b we have to combine n_{tot} in Equations A1.2–3, the partition coefficients and Equation A1.7. Then we have:

$$C_{aq} = \frac{C_b}{MW \cdot \left(\frac{f_{aq}}{\rho_{aq}} + \frac{f_L}{\rho_L} K_L + \frac{f_p}{\rho_p} K_p \right)} \quad (A1.8)$$

where f_i refers to the mass fraction of each compartment (aqueous, lipid, proteins) in the cell. Replacing this equation into Equation A1.5 and rearranging we obtain:

$$\frac{dC_b}{dt} = \left(\frac{MW \cdot V^{2/3}}{W} r_{da} \right) C_{diss} - \left(\frac{V^{2/3}}{W \left(\frac{f_{aq}}{\rho_{aq}} + \frac{f_L}{\rho_L} K_L + \frac{f_p}{\rho_p} K_p \right)} r_{ad} \right) C_b - \left(\frac{1}{W} \frac{dW}{dt} \right) C_b \quad (A1.9)$$

The last term can be neglected in the case of HepaRG cells. Equation A1.9 gives the concentration inside of the cell from outside concentration and the chemical concentration in the liver obtained from PBKT model. C_{diss} stands for concentrations in the liver calculated by the PBTK model. The direct effects of a chemical concentration, C , on survival may be expressed by:

$$\frac{dn}{dt} = -kt \cdot (C_b - NEC) \cdot n \quad (A1.10)$$

where n is the number of cells, kt is the killing rate and NEC is the No Effect Concentration. C_b is the same term in Equation A1.9. Equation A1.10 is appropriate in the case of HepaRG cells since cell cycle has only one step.

In this way the joint PBTK-VCB modelling (PBTK model: liver compartment + VCB: Equations A1.9–10 can predict, in the long run, the liver cell viability–dose relationship.

References

- Barter, Z.E., Bayliss, M.K., Beaune, P.H., Boobis, A.R., Carlile, D.J., Edwards, R.J., et al., 2007. Scaling factors for the extrapolation of in vivo metabolic drug clearance from in vitro data: reaching a consensus on values of human microsomal protein and hepatocellularity per gram of liver. *Curr. Drug Metab.* 8, 33–45.
- Billoir, E., Péry, A.R.R., Charles, S., 2007. Integrating the lethal and sublethal effects of toxic compounds into the population dynamics of *Daphnia magna*: a combination of the DEBtox and matrix population models. *Ecol. Modell.* 203, 204–214.
- Bronaugh, R.L., Franz, T.J., 1986. Vehicle effects on percutaneous absorption: in vivo and in vitro comparisons with human skin. *Br. J. Dermatol.* 115, 1–11.
- Carrier, O., Pons, G., Rey, E., Richard, M.-O., Moran, C., Badoual, J., et al., 1988. Maturation of caffeine metabolic pathways in infancy. *Clin. Pharmacol. Ther.* 44, 145–151.
- Chambin-Remoussenard, O., Treffel, P., Bechtel, Y., Agache, P., 1993. Surface recovery and stripping methods to quantify percutaneous absorption of caffeine in humans. *J. Pharm. Sci.* 82, 1099–1101.
- Csajka, C., Haller, C.A., Benowitz, N.L., Verotta, D., 2005. Mechanistic pharmacokinetic modelling of ephedrine, norephedrine and caffeine in healthy subjects. *Br. J. Clin. Pharmacol.* 59, 335–345.
- Dias, M., Farinha, A., Faustino, E., Hadgraft, J., Pais, J., Toscano, C., 1999. Topical delivery of caffeine from some commercial formulations. *Int. J. Pharm.* 182, 41–47.
- Dimitrov, S.D., Low, L.K., Patlewicz, G.Y., Kern, P.S., Dimitrova, G.D., Comber, M.H.I., et al., 2005. Skin sensitization: modeling based on skin metabolism simulation and formation of protein conjugates. *Int. J. Toxicol.* 24, 189–204.
- Doucet, O., Ferrero, L., Garcia, N., Zastrow, L., 1998. O/W emulsion and W/O/W multiple emulsion: physical characterization and skin pharmacokinetic comparison in the delivery process of caffeine. *Int. J. Cosmet. Sci.* 20, 283–295.
- Feldmann, R.J., Maibach, H.I., 1970. Absorption of some organic compounds through the skin in man. *J. Invest. Dermatol.* 54, 399–404.
- Franz, T.J., 1978. The finite dose technique as a valid in vitro model for the study of percutaneous absorption in man. *Curr. Probl. Dermatol.* 7, 58–68.
- Gajewska, M., Worth, A., Urani, C., Briesen, H., Schramm, K., 2014. Application of physiologically-based toxicokinetic modelling in oral-to-dermal extrapolation of threshold doses of cosmetic ingredients. *Toxicol. Lett.* 227.
- Gérard, C., Goldbeter, A., 2009. Temporal self-organization of the cyclin/Cdk network driving the mammalian cell cycle. *Proc. Natl. Acad. Sci. U.S.A.* 106, 21643–21648.
- Ginsberg, G., Hattis, D., Russ, A., Sonawane, B., 2004. Physiologically based pharmacokinetic (PBPK) modeling of caffeine and theophylline in neonates and adults: implications for assessing children's risks from environmental agents. *J. Toxicol. Environ. Health Part A* 67, 297–329.
- Ha, H.R., Chen, J., Krähenbühl, S., Follath, F., 1996. Biotransformation of caffeine by cDNA-expressed human cytochromes P-450. *Eur. J. Clin. Pharmacol.* 49, 309–315.
- Herman, A., Herman, A.P., 2012. Caffeine's mechanisms of action and its cosmetic use. *Skin Pharmacol. Physiol.* 26, 8–14.
- Lehman, P.A., Raney, S.G., Franz, T.J., 2011. Percutaneous absorption in man: in vitro-in vivo correlation. *Skin Pharmacol. Physiol.* 24, 224–230.
- Lelo, A., Birkett, D.J., Robson, R.A., Miners, J.O., 1986. Comparative pharmacokinetics of caffeine and its primary demethylated metabolites paraxanthine, theobromine and theophylline in man. *Br. J. Clin. Pharmacol.* 22, 177–182.
- Liu, X., Grice, J.E., Lademann, J., Otberg, N., Trauer, S., Patzelt, A., et al., 2011. Hair follicles contribute significantly to penetration through human skin only at times soon after application as a solvent deposited solid in man. *Br. J. Clin. Pharmacol.* 72, 768–774.
- Lopes, C., Péry, A.R.R., Chaumont, A., Charles, S., 2005. Ecotoxicology and population dynamics: using DEBtox models in a Leslie modeling approach. *Ecol. Modell.* 188, 30–40.
- Lotte, C., Wester, R.C., Rougier, A., Maibach, H.I., 1993. Racial differences in the in vivo percutaneous absorption of some organic compounds: a comparison between black, Caucasian and Asian subjects. *Arch. Dermatol. Res.* 284, 456–459.
- Mennecozzi, M., Landesmann, B., Harris, G.A., Liska, R., Whelan, M., 2011. Hepatotoxicity screening taking a mode-of-action approach using HepaRG cells and HCA. *Altox Proc.* 1/12, WC8.
- Moré, J.J., 1978. The Levenberg-Marquardt algorithm: implementation and theory. *Lect. Notes Math.* 630, 105–116.
- Newton, R., Broughton, L.J., Lind, M.J., Morrison, P.J., Rogers, H.J., Bradbrook, I.D., 1981. Plasma and salivary pharmacokinetics of caffeine in man. *Eur. J. Clin. Pharmacol.* 21, 45–52.
- OECD SIDS, 2002. Caffeine: SIDS initial assessment report for SIAM 14.
- Otberg, N., Patzelt, A., Rasulev, U., Hagemester, T., Linscheid, M., Sinkgraven, R., et al., 2008. The role of hair follicles in the percutaneous absorption of caffeine. *Br. J. Clin. Pharmacol.* 65, 488–492.
- Regal, K.A., Kunze, K.L., Peter, R.M., Nelson, S.D., 2005. Oxidation of caffeine by CYP1A2: isotope effects and metabolic switching. *Drug Metab. Dispos.* 33, 1837–1844.
- Roskos, K.V., Maibach, H.I., Guy, R.H., 1989. The effect of aging on percutaneous absorption in man. *J. Pharmacokin. Biopharm.* 17, 617–630.
- Venkatakrishnan, K., Von Moltke, L.L., Court, M.H., Harmatz, J.S., Crespi, C.L., Greenblatt, D.J., 2000. Comparison between cytochrome P450 (CYP) content and relative activity approaches to scaling from CDNA-expressed CYPs to human liver microsomes: ratios of accessory proteins as sources of discrepancies between the approaches. *Drug Metab. Dispos.* 28, 1493–1504.
- Wilkinson, S.C., Maas, W.J.M., Nielsen, J.B., Greaves, L.C., van de Sandt, J.J.M., Williams, F.M., 2006. Interactions of skin thickness and physicochemical properties of test

- compounds in percutaneous penetration studies. *Int. Arch. Occup. Environ. Health* 79, 405–413.
- Zaldívar, J.M., Mennecozi, M., Marcelino Rodrigues, R., Bouhifd, M., 2010. A biology-based dynamic approach for the modelling of toxicity in cell-based assays. Part I: fate modelling.
- Zaldívar, J.M., Mennecozi, M., Macko, P., Rodriguez, R., Bouhifd, M., Baraibar Fentanes, J., 2011. A biology-based dynamic approach for the modelling of toxicity in cell assays. Part II: models for cell population growth and toxicity.
- Zandvliet, A.S., Huitema, A.D.R., De Jonge, M.E., Den Hoed, R., Sparidans, R.W., Hendriks, V.M., et al., 2005. Population pharmacokinetics of caffeine and its metabolites theobromine, paraxanthine and theophylline after inhalation in combination with diacetylmorphine. *Basic Clin. Pharmacol. Toxicol.* 96, 71–79.